

# Development of a 45 GHz Multiple-Beam Antenna for Military Satellite Communications

K. Sudhakar Rao, *Member, IEEE*, Gilbert A. Morin, *Member, IEEE*,  
Minh Q. Tang, Sylvain Richard, *Member, IEEE*, and Kwok Kee Chan

**Abstract**—Design and experimental results of a wide-angle coverage 45 GHz multiple-beam antenna for military satellite communications are presented in this paper. The high-gain spot beams with low sidelobe levels and efficient adjacent beam overlap are generated by employing an offset parabolic reflector with overlapping feed clusters. The beam shape can be adapted to cancel either single- or multiple-jammers by varying excitations within the feed cluster corresponding to the beam. Development of antenna components including Potter horn, polarizer, phase-amplitude controller, and beamforming network is discussed. Measured results of the demonstration antenna have shown that sidelobe and crosspolar levels of better than  $-25$  dB are achieved for beams scanned over an eight-degree diameter circular coverage region. The adapted patterns of the antenna agree well with the computations, and null depths of better than 30 dB have been realized over a 4.5% bandwidth.

## I. INTRODUCTION

A multiple-beam satellite system is being considered by the Canadian Department of National Defence (DND) for future military communications. The satellite will be operated at EHF frequencies (45/20 GHz links) with high-gain spot beams of one-degree diameter footprints contiguously covering the service region. These beams are circularly polarized and are required to have an adjacent beam overlap of about 3 dB. To provide a reliable performance, the receive multiple-beam antenna (MBA) must have low sidelobe and crosspolar levels of better than  $-25$  dB to reduce the effects of interference and jamming [1], [2].

Stein [3] has shown that for any MBA with overlapped beams, cross coupling between the feed lines is unavoidable, and as a result, efficiency values of only 50% or less are achievable. Dufort [4] has verified that Stein's efficiency limit can be achieved by placing attenuation in the aperture of a Butler matrix in accordance with the aperture distribution. Most of the previous work on MBA's is limited to orthogonal beams and linear arrays. The scope of the present paper extends to nonorthogonal beams with two-dimensional beam stacking that can be adapted for various jammers.

Manuscript received November 1, 1993; revised April 13, 1995. This work was supported in part by the Department of National Defence, Canada, under Contract W 8477-8-TB04/01-SV.

K. S. Rao, M. Q. Tang, and S. Richard are with Spar Aerospace Limited, Ste-Anne-de-Bellevue, Québec, Canada H9X 3R2.

G. A. Morin is with the Defence Research Establishment, Ottawa, Ontario, Canada K1A 0Z4.

K. K. Chan is with Chan Technologies Incorporated, Kirkland, Canada H9H 3V3.

IEEE Log Number 9414060.

The fundamental objective for any MBA is to maximize the minimum gain within the coverage region. If the MBA has uniform beams arranged in a hexagonal grid fashion, the minimum gain occurs at the triple beam crossover of the adjacent beams, and the variation within the coverage region is typically around 4 dB. The trades for gain optimization are often coupled with considerations such as sidelobe levels and hardware complexity. The basic antenna concepts for multiple beam generation are a) single-aperture design and b) multiple-aperture design. Fig. 1 illustrates both the MBA concepts. The multiple aperture design can employ two, three, or four independent apertures (reflectors or lenses), where adjacent beams are generated by different apertures forming an interleaved spot beam coverage on ground. The closest spacing that occurs between beams produced by adjacent feed horns from the same aperture can be increased to  $1.414\Theta_0$ ,  $1.73\Theta_0$ , and  $2.0\Theta_0$  ( $\Theta_0$  is the half-power beamwidth) for two, three, and four aperture designs, respectively. The larger beam spacing allows the increase of the horn size to improve the antenna gain through reduced spillover and also to reduce the sidelobe levels. The Military Strategic Tactical and Relay (MILSTAR) is the latest satellite payload which employs multiple dielectric lenses for the transmit (20 GHz) and receive (44 GHz) antennas [5]. The receive MBA consists of four interleaved lenses to provide global coverage. Disadvantages associated with multiple aperture systems are the spacecraft real estate and coverage distortions due to pointing error differences from various apertures.

Single-aperture MBA's can be implemented using either lens or reflector designs. Lens designs with single apertures are less attractive compared to reflector designs due to mechanical and electrical implications. The mass would be at least twice that of an equivalent reflector system. Therefore, only reflector designs are selected for the single-aperture MBA trade-offs. Due to the low sidelobe requirements, only offset reflector configurations are considered suitable for this development. Ingerson and Chen [6] explored the possibility of using a nonfocusing reflector such as an offset hyperboloid to realize multiple-spot beams. The main disadvantages of the hyperbolic reflector MBA's are that they require very large apertures, pattern distortion for scanned beams due to increased defocusing effects, and increased sidelobe and crosspolar levels.

The single-aperture MBA utilizes an offset paraboloid feed by an array of primary radiating elements located along the focal-plane of the reflector. The design trade-off is the type of feed mechanism required to achieve good efficiency, beam

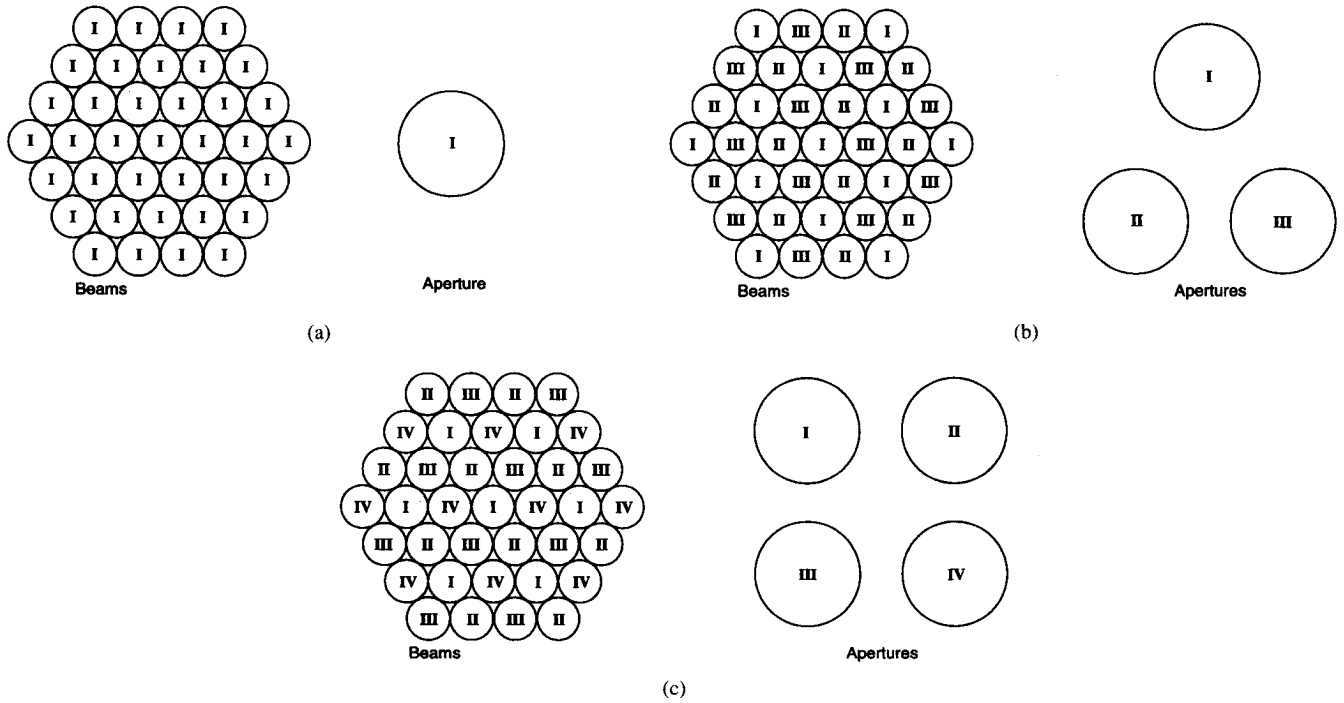


Fig. 1. Aperture concepts for multiple-beam antennas: (a) single-aperture antenna, (b) three-aperture antenna, and (c) four-aperture antenna.

overlap, and low sidelobe and crosspolar levels. Two types of feed mechanisms that are possible with this design are:

- Basic feed concept
- Enhanced feed concept.

Fig. 2 illustrates the two feed concepts for the MBA. The “basic feed concept” utilizes a single horn per beam to generate the multiple beams. This design gives beam peak gain values which are typically 2–3 dB lower than that which could be achieved using a single optimum horn size. This is due to the fundamental limitation of the antenna which requires a larger feed size to increase the antenna gain and smaller feed to improve the beam overlap. The relationship between the beam overlap and antenna efficiency as a function of horn size is given in Table I. It is seen from these results that the design which meets the 3 dB beam overlap has high sidelobe levels of  $-19$  dB relative to peak gain and an antenna efficiency of 48%. This value compares very closely with Stein’s efficiency limit of 50% for MBA’s with simple feeds [3]. On the other hand, a low sidelobe design of  $-30$  dB has 70% antenna efficiency but an adjacent beam overlap of 23 dB. It is evident from the above results that the “basic feed concept” cannot simultaneously meet the low sidelobe and high adjacent beam overlap requirements of the MBA.

The “enhanced feed concept” utilizes a cluster of horns instead of a single horn to generate each beam. The composite beams of this MBA can be simultaneously generated within the coverage region at beam locations corresponding to the individual component beams. A septet array with six elements forming a circular ring around a central element (see Fig. 2) is considered as a good choice for the MBA. This is due to the fact that the septet array can control the sidelobe levels all around the main beam ( $\Theta = 0$  to 360 degrees). This concept

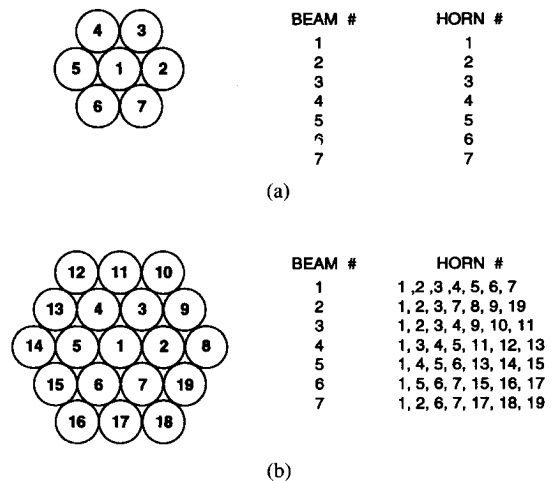


Fig. 2. Illustration of feed concepts (a) basic feed concept using single horn per beam and (b) enhanced feed concept using septet horn array per beam.

has more degrees-of-freedom compared to the “basic feed concept” for simultaneous optimization of various performance parameters of the MBA. For example, the excitations within the septet array forming a composite beam can be varied to achieve low sidelobe levels as well as good overlap between adjacent beams. This is feasible because of the virtual increase in the element size for a given interelement spacing. Also, the septet array excitations can be varied to adapt the beam to cancel up to six jammers.

The operational antenna requires about 70 beams and 121 elements to cover an eight-degree diameter circular coverage with approximately one-degree overlapping beams. The sidelobe and crosspolar levels need to be better than  $-25$  dB to

TABLE I  
BEAM OVERLAP VERSUS SIDELOBE LEVELS OF THE  
REFLECTOR MBA USING SINGLE HORN PER BEAM\*

HORN SIZE ( $d/\lambda$ )	BEAM OVERLAP (-dB)	PEAK SIDELOBE LEVEL (-dB)	ANTENNA EFFICIENCY (%)
0.7	1.84	18.4	40.0
0.9	2.80	18.8	43.8
1.1	4.00	19.2	52.8
1.3	5.60	20.0	55.9
1.5	7.20	20.4	65.0
1.7	9.60	21.2	71.9
1.9	12.00	22.2	76.6
2.1	14.80	23.4	78.9
2.3	17.60	24.2	79.1
2.5	20.00	26.0	76.7
2.7	22.40	28.0	72.9
2.9	24.00	36.0	67.9
3.1	25.20	41.0	61.9

\* The above results are with  $F/D$  ratio of the reflector as 0.8. The results can be generalized for any  $F/D$  ratio by changing the first column by  $(d/\lambda)_{new} = 1.25(d/\lambda) \cdot (F/D)$ .

minimize the interference due to jammers. The beamforming network (BFN) for the operational antenna will be realized at low-level (after LNA's) where the losses are not critical. It will be implemented using microstrip technology.

An exploratory multiple-beam antenna (XMBA) has been designed, fabricated, and tested with the objective of simulating the electrical performance of the operational system. The XMBA has seven elements to form a single composite beam, and the operational MBA performance is tested by moving the feed array along the focal-plane of the reflector. The BFN for the XMBA is designed with waveguide technology which is quite different from the operational antenna BFN. Measured results of the XMBA have shown that low sidelobe and crosspolar levels of better than  $-27$  dB are achieved in conjunction with high adjacent beam overlap of 2.8 dB. Adapted patterns of the XMBA have also been measured for different jamming scenarios, and the measured patterns compare well with theoretical simulations.

## II. MBA DESIGN

A single-aperture offset parabolic reflector antenna being fed with a focal-plane feed array has been selected for the MBA. The reflector is fed with overlapping feed clusters, whereby each beam is generated using a septet array. Element beam approach is used for nulling which employs individual horn weights (amplitude and phase) within the septet as variables to adapt the composite beam shape.

### A. Design Trade-Offs

Various design parameters which influence the electrical performance of the offset parabolic reflector antenna are discussed below. Design equations relating the electrical performance to the antenna parameters are given based on approximate analyses.

**Antenna Size:** The size of the antenna depends on the beamwidth and the sidelobe-level requirements. Reflector di-

ameter ( $D$ ) related to the beamwidth and sidelobe level is given as [7]

$$D = (33.2 - 1.55S_L)\lambda/\Theta_0 \quad (1)$$

where  $S_L$  is the peak sidelobe level (-dB) relative to peak gain,  $\Theta_0$  is the half power beamwidth, and  $\lambda$  is the wavelength. The reflector size is also determined based on the sidelobe isolation required over the specified angular region which is the angular distance between the edge of the main beam and the skirt region ( $\Delta\Theta_L = (3\Theta_0 - \Theta_0)/2 = \Theta_0$ ). Minimum size of the reflector related to  $\Delta\Theta_L$  and  $S_L$  is given as [7]

$$D_{min} = (3.74 - 2.55S_L)\lambda/\Delta\Theta_L. \quad (2)$$

The reflector sizes based on one-degree beamwidth and  $-30$  dB sidelobe levels are obtained from (1) and (2) as 21.64 and 21.79 in, respectively. The projected aperture diameter of the offset paraboloid is chosen as 22 in.

**Focal Length:** The focal length ( $F$ ) is usually chosen such that the  $F/D$  ratio is in the range 0.8–1.4. A large  $F/D$  gives better scan performance of the MBA and also better crosspolar performance of the antenna. For small  $F/D$  values, the scan performance of the MBA deteriorates, and also the radiation patterns deteriorate due to increased mutual coupling effects caused by the small electrical size of the feed element ( $d \simeq 0.8\lambda$ ). An  $F/D$  ratio of 1.68 which corresponds to a focal length of 37 in is found optimum for this antenna.

**Offset Clearance:** The offset clearance of the reflector is mainly dictated by the need to avoid geometrical blockage from the feed array and the spacecraft structure. For the MBA, the geometrical blockage due to the feed array for beams scanned to the edge of coverage region ( $\Theta_S = \pm 4$  degrees) must be avoided to realize the coverage gain and low sidelobe performance. A 5.9 in offset clearance is selected such that an adequate angular separation of 4.3 degrees is maintained between the antenna boresight and the line joining the reflector edge and the closest feed element.

**Number of Elements:** The number of feed elements depends on the coverage area and the antenna size and is approximately given as [8]

$$N \simeq \text{coverage area (in square degrees)} / [2746(\lambda/D)^2]. \quad (3)$$

The denominator in the above expression represents the area of the hexagon circumscribed by the constituent beams. The coverage area is usually larger than the geographical area and includes pointing error of the antenna. For a circular coverage of eight-degree diameter and with  $D/\lambda = 82.89$ , the number of feed elements  $N$  from (3) is 126. The feed array selected has 121 radiating elements.

**Radiating Element:** The choice of the radiating element and its size are the key factors in determining the overall performance of the MBA. The size of the element depends on the  $F/D$  ratio and is given approximately as

$$d/\lambda \simeq 1.25(F/D). \quad (4)$$

For the selected  $F/D$  ratio of 1.682, the horn size is approximately  $2.1\lambda$ . The design of the radiating element is dictated

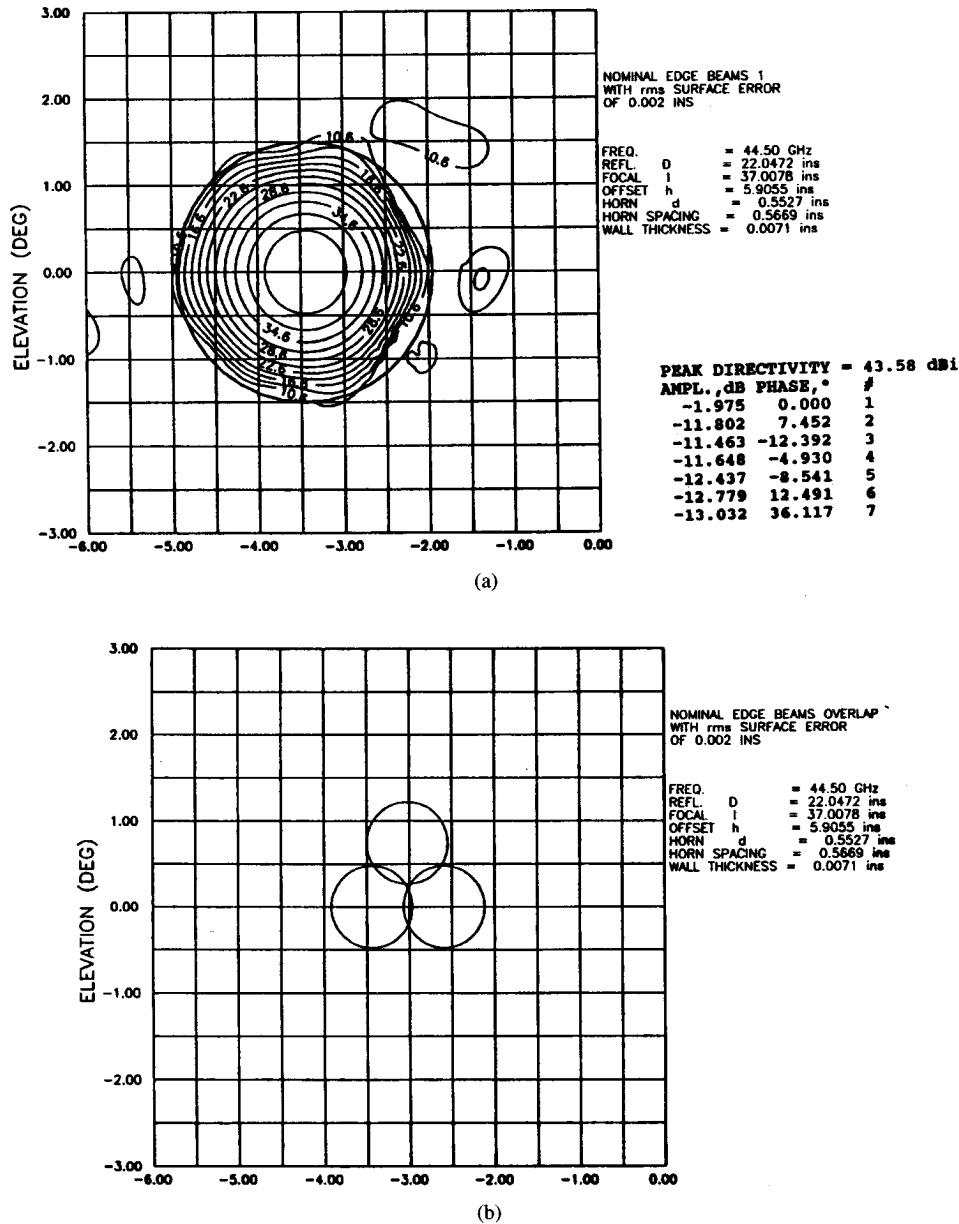


Fig. 3. (a) Computed copolar directivity contours of the composite beam for worst-case scan; (b) 3-dB directivity contours of edge beams showing the beam overlap.

by the low crosspolar requirements of the MBA. Since the offset reflector does not generate any crosspolar component for circular polarization, the main sources of crosspolarization are the radiating element and polarizer. The on-axis crosspolar levels of the antenna are caused by the polarizer, while the off-axis crosspolar levels are due to the horn. The dominant  $TE_{11}$  mode circular horn has high crosspolar levels of the order of  $-20$  dB for an aperture diameter of  $2.1\lambda$ , while the hybrid  $HE_{11}$  mode corrugated horn has poor overlap between adjacent beamlets of the MBA due to thick walls. A dual-mode Potter horn with  $TE_{11}$  and  $TM_{11}$  modes of propagation is selected for this antenna.

**B. MBA Performance Computations**

The antenna comprises a 22-in diameter offset parabolic reflector fed with a focal-plane array. The feed array consists

of 121 Potter horns, each with a 0.553-in aperture arranged in a hexagonal grid. Size of the feed array is 6.80 in  $\times$  6.46 in. The offset angle  $\Theta_0$  for the feed array is selected as 25.48 degrees. The composite beam directivity gain contours are simulated using a septet array with no individual beam overlap requirement. Element patterns are modeled as Potter horn primary radiation. Secondary patterns of the antenna are synthesized using TICRA's GRASP 7 software by first computing and storing all the seven secondary patterns due to individual elements of the septet array. Desired pattern is then specified for the optimization routine as discrete data in the main beam as well as the sidelobe region outside the skirt area (three-degree diameter circle with center as the main beam peak). The amplitude and phase excitations of the septet array are optimized using the mini-max routine. The composite beam directivity contours are then computed by

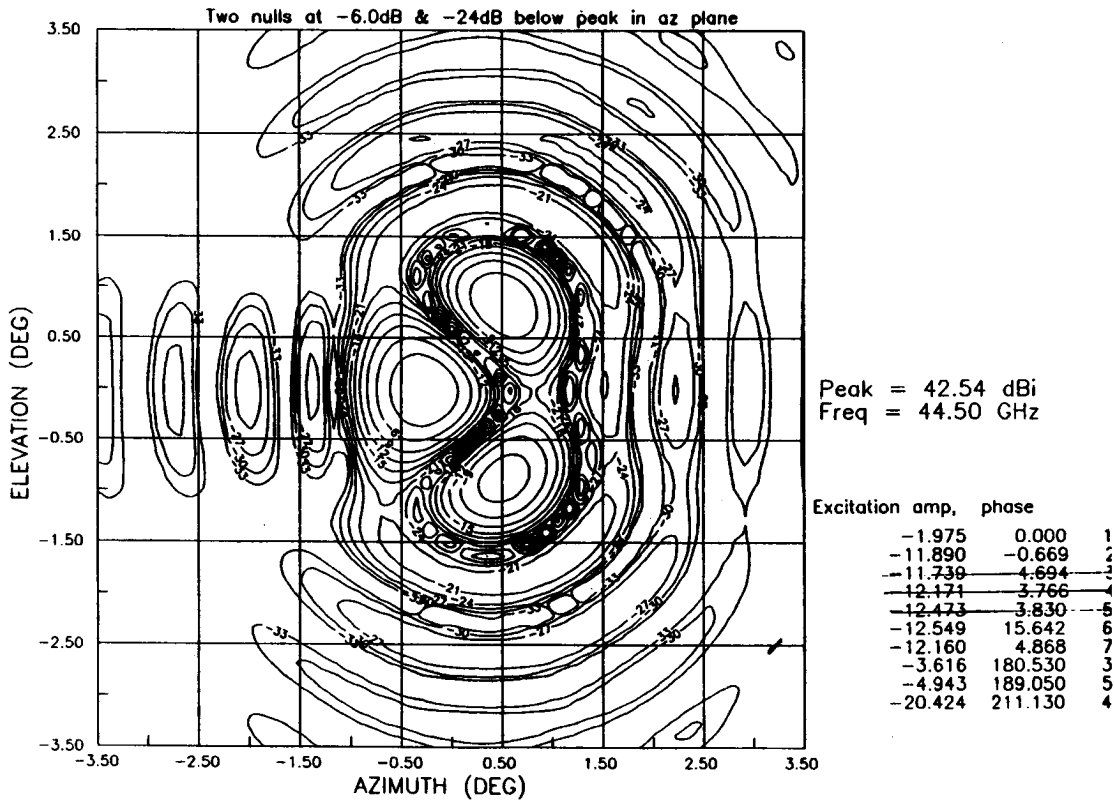


Fig. 4. Computed directivity contour plot of the adapted beam for two jammers located in the main beam skirt region at -6 dB and -24 dB relative to peak of composite beam.

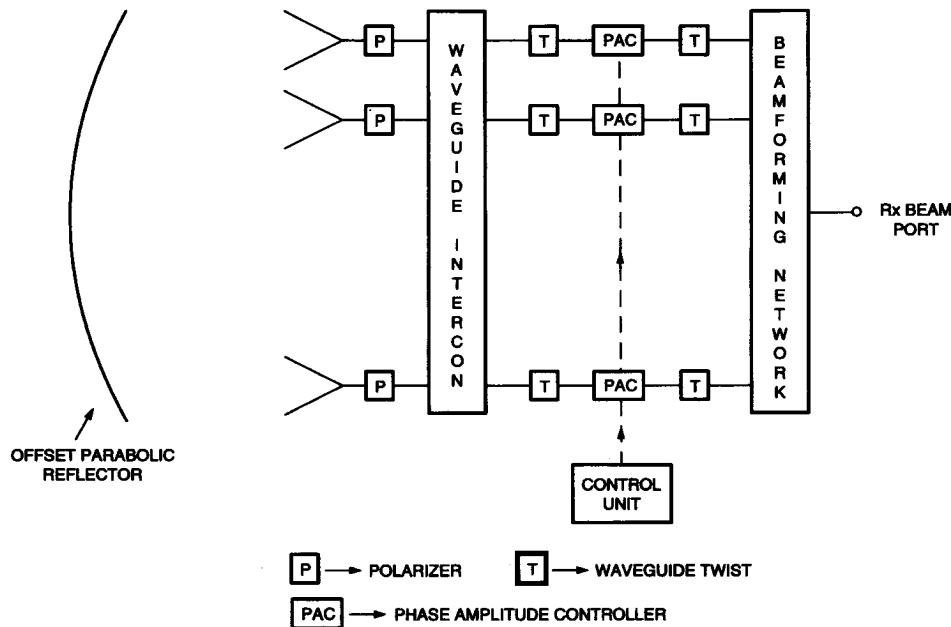


Fig. 5. Block diagram of the XMBA.

weighting the stored individual beamlet directivity values with optimized excitations and summing them up. The computed electrical performance of the antenna includes the following fabrication tolerances and imperfections:

- Rms surface error of the reflector,
- Finite wall thickness of the horns, and
- On-axis axial ratio due to polarizers.

An rms surface error of 0.002 in ( $\lambda/130$ ) has been specified for the manufacturing of the reflector and has been used in the computations. This surface error will cause gain degradation of approximately 0.05 dB and sidelobe increase of about 0.3 dB [9].

Fig. 3(a) shows the computed directivity contours of the worst-case edge beam using optimized excitations of the septet

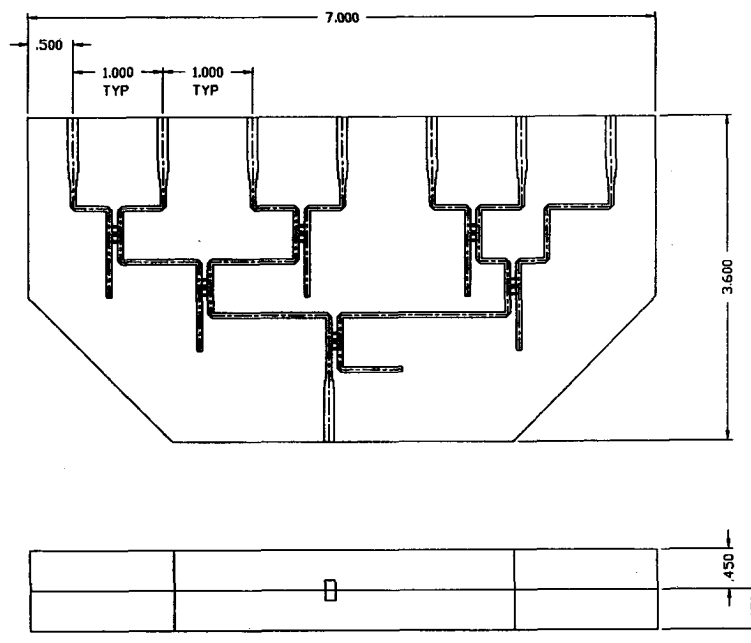


Fig. 6. Layout of the beamforming network.

array. Worst-case sidelobe levels outside the skirt region are computed as  $-29.7$  dB relative to peak gain. The synthesized 3 dB directivity contours of adjacent composite beams close to the edge of coverage arc shown in Fig. 3(b). An adjacent composite beam overlap of 2.8 dB and a triple beam overlap of 3.1 dB has been computed for this MBA design. The computed crosspolar gain contours with 0.4 dB on-axis axial ratio due to the feed indicate that crosspolar levels are lower than  $-33$  dB relative to peak gain.

Adapted patterns of the MBA are computed for different jamming scenarios using the element beam approach. The amplitude and phase weightings of the septet array to create a null or multiple nulls in the adapted patterns for given jammer location(s) are determined as follows: amplitude and phase values of the far-field secondary patterns of individual elements of the septet array are computed initially, the weights of the closest elements of the septet to the jammer location(s) are only adjusted to create a single or multiple nulls; the weights of the remaining elements are unchanged from the optimal composite beam excitations; the far-field gain matrices of individual horns are weighted according to optimized excitations, and the resultant adapted pattern is thus computed. This particular scheme allows for graceful degradation of the adapted beam gain over the main beam region. Adapted pattern contours for two jammers located in the main beam skirt region at  $-6$  and  $-24$  dB levels relative to peak of the composite beam are shown in Fig. 4. They have been computed by changing the excitations of three elements (#3, 4, and 5). Minimum null depth of 35 dB has been computed for the adapted beam.

### III. XMBA HARDWARE DEVELOPMENT

An XMBA has been breadboarded to demonstrate the electrical performance of the receive MBA for the EHF



Fig. 7. Photograph of the XMBA assembly in the compact range facility.

Satcom. It consists of an offset parabolic reflector (having geometrical dimensions as those given in Section II) being fed with a septet array to produce one composite beam. The scanned beam performance of the XMBA is measured by moving the septet feed array in the focal plane of the reflector. Fig. 5 shows the block diagram of the XMBA. The feed array consists of seven Potter horns, polarizers, waveguide interconnecting network, phase amplitude control (PAC) devices, a control unit, and a 7-1 passive combiner. The required amplitude and phase excitations of the elements of the septet are realized through PAC devices and the control processor.

#### A. Reflector

The reflector is fabricated by machining the required surface from a block of aluminum. Reflector surface is heat treated for

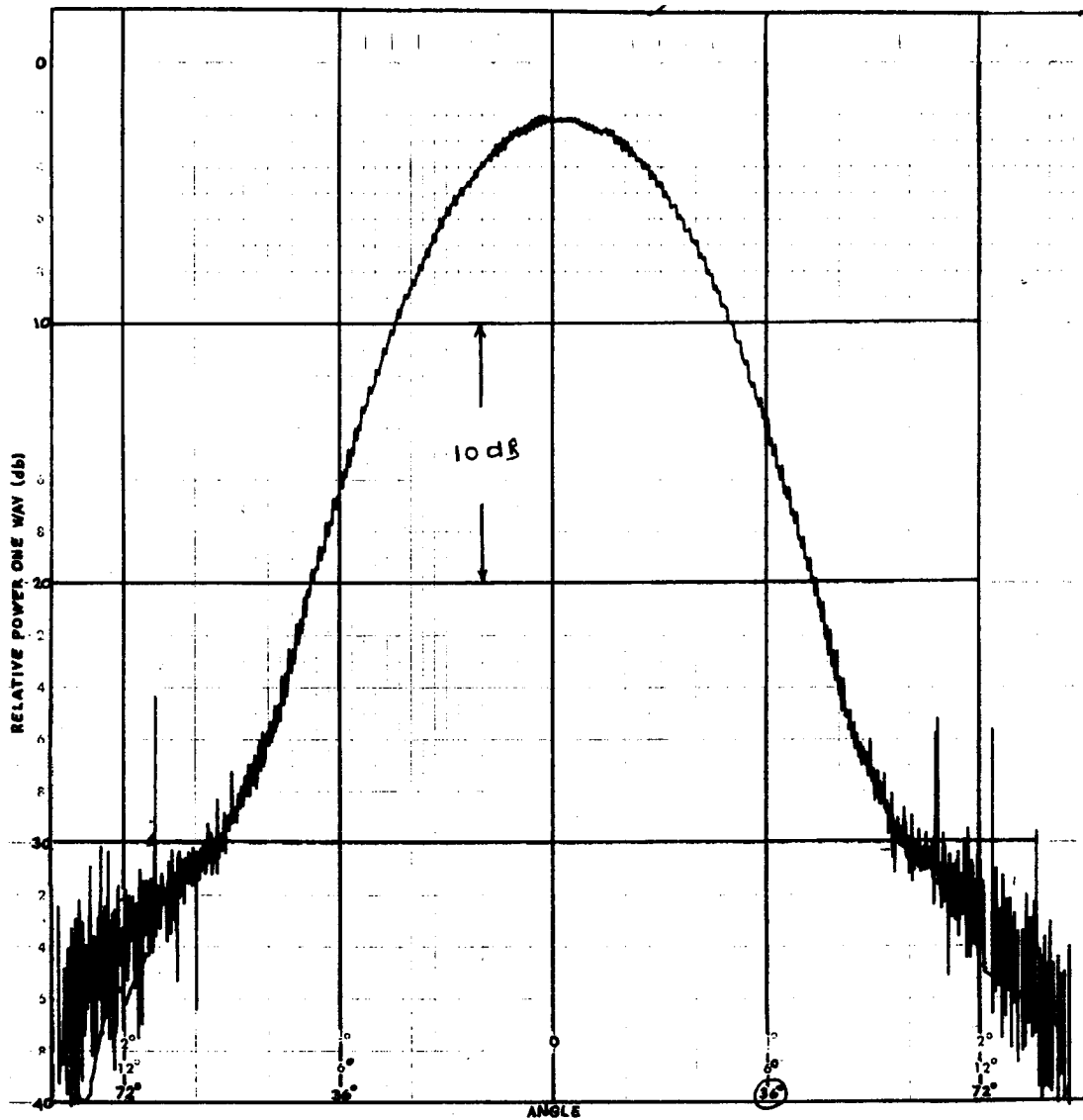


Fig. 8. Measured circularly polarized radiation patterns of the Potter horn.

stress relieving prior to final surface machining. The reflector is bolted to a small wedge-shaped back-up structure designed to align the reflector and the feed array in the correct positions for the testing. The measured rms surface error of the fabricated reflector is 0.0011 in.

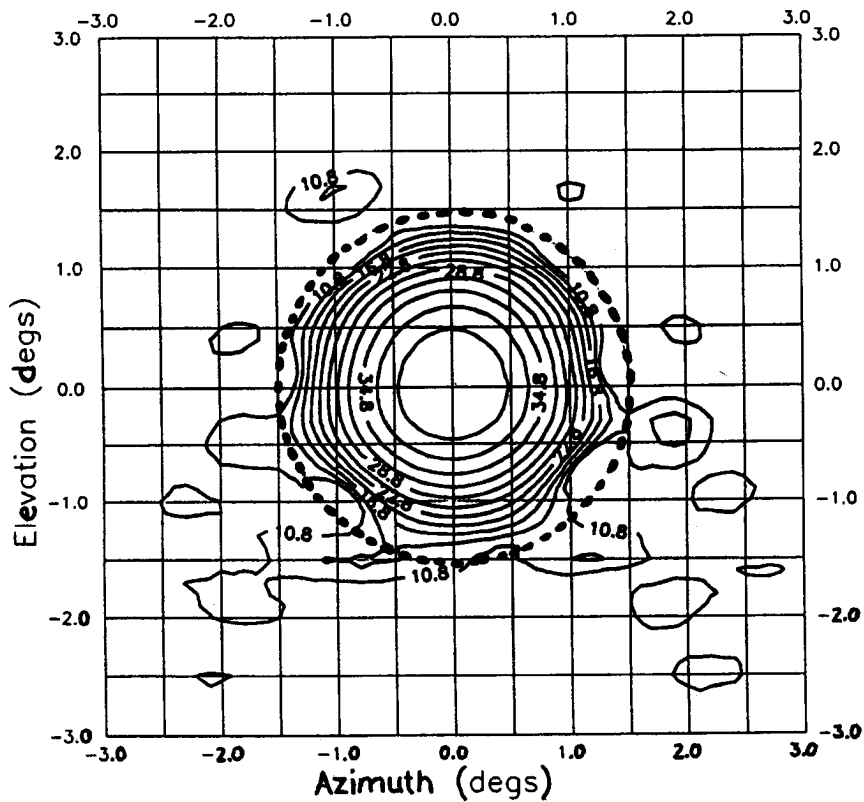
### B. Horn Array

The horn array consists of seven circularly polarized radiating elements which are closely packed in a hexagonal grid configuration with neighboring elements touching each other at the aperture. Each radiating element consists of a Potter horn, a pin polarizer, a transformer, and a WR22 rectangular waveguide. The Potter horn is realized using two flared sections. A waveguide transformer is implemented in the horn to provide an impedance match between the 0.236-in diameter and 0.189-in diameter circular waveguides. The geometrical parameters of the horn have been optimized through a MINIMAX software which employs an analysis

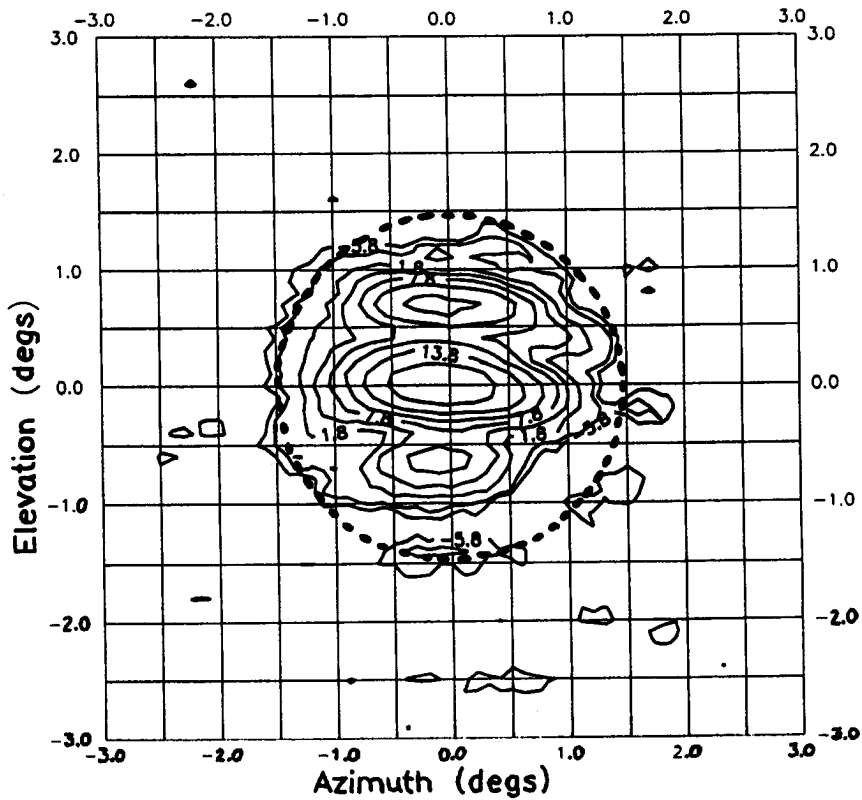
routine based on mode-matching technique [10]. The polarizer is realized in the 0.189-in circular waveguide using 11 pairs of pins. Spacing between successive pins is 0.040 in. Depths of each pair of screws is gradually varied to obtain the 90-degree phase shift between horizontal and vertical field vectors over the band and also to achieve good return loss (better than 30 dB). The output of the polarizer is connected to a transformer section to match the circular waveguide (0.189-in diameter) impedance to WR22 rectangular waveguide impedance.

### C. Waveguide Intercon Assembly

The intercon assembly provides the RF path between the horn array and the PAC modules. It transforms the dense cluster of horns (input ports) into a linear array of output ports. The interconnecting network is realized as an integrated waveguide assembly. Using this technology, the waveguide channels and bends are milled integrally as two mirror-image solid pieces of aluminum. A planar waveguide network is



(a)



(b)

Fig. 9. Measured gain contours of the XMBA central beam: (a) copolar, (b) crosspolar.

then formed by assembling the two mirror-image halves. The overall size of the intercon assembly is about 8 in × 4 in ×

0.9 in. The horn assembly sits on top of the intercon box. The output ports of the intercon assembly are connected to the PAC

units via seven discrete 90-degree waveguide (WR22) twists. The twists are short sections of waveguide (about 1.5 in long) which progressively rotate the waveguides about their axes of propagation. Twists are needed since the PAC module input ports and the intercon assembly output ports are perpendicular to each other.

#### D. PAC Assembly

The PAC module combines the functions of variable attenuator and variable phase shifter into a single device. It consists of an input 3-dB coupler which splits the input signal into two equal components that are routed through two ferrite variable phase shifters (VPS). This allows independent phase adjustment of the two signal components. The signals are then recombined using an output coupler. The output of the coupler is the vector sum of the two signals. The amplitude control is achieved by setting the differential phase of the VPS's properly, while the phase is controlled by varying the phase of both VPS's by a common value. The PAC module has an amplitude variation of 0–30 dB and a phase variation of 0–360 degrees over the 43.5–45.5 GHz band and a switching speed of 15 microseconds.

The control electronics for the PAC modules consists of an interface electronics for the parallel control bus and drivers to generate the current pulses for the PAC modules. The PAC module assembly is controlled by an IBM compatible computer which allows for sequential control of the 7 PAC modules by interactively entering the PAC number (1–7), attenuation (0–30 dB), and phase (0–360 degrees). The PAC assembly and the associated software were developed by the Electromagnetic Sciences (EMS), Atlanta.

#### E. Beamforming Network (BFN)

The function of the BFN is to combine the seven outputs of the PAC modules uniformly. It is a passive 7–1 combiner realized using integrated waveguide technology. Four types of components are used for the passive BFN assembly, namely branchline couplers, dummy loads, bends, and transformers. The branchline couplers are realized in reduced height WR22 waveguide (0.060 in  $\times$  0.224 in internal dimensions) with three branches whose gap sizes vary from 0.020–0.065 in. The unused port of the couplers are terminated with Eccosorb MF117 loads. Ninety-degree E-plane bends with miter compensation are used for routing the waveguide channels. The manufacturing process of the BFN is similar to the intercon assemble, namely, NC milling with probe EDM. The layout of the BFN is shown in Fig. 6. The fabricated BFN assembly has overall dimensions of 7.0 in  $\times$  3.6 in  $\times$  0.9 in.

The BFN for the operational MBA is more complicated than the XMBA BFN. This is due to the fact that the signal from each element needs to be divided into seven ways to share among seven beams and signals from seven adjacent elements are then combined to form the simultaneous beams. The BFN will be implemented at low-level (after LNA's) where losses are not critical using a series-series type (similar to Blass Matrix) BFN realized using printed technology.

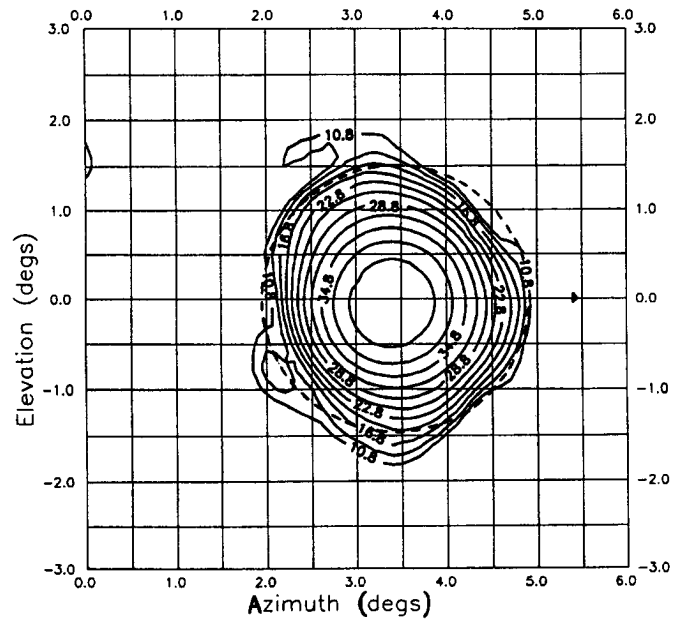


Fig. 10. Measured copolar gain contour of the edge scanned beam.

#### F. XMBA Assembly

The photograph of the XMBA assembly is shown in Fig. 7. The offset reflector and the feed assembly are mounted on an L-shaped frame structure which is designed to sit on a turntable using a dolly structure. Mounting facilities for the reflector include a wedge-shaped fixture designed to align the reflector. The feed assembly is fixed to an aluminum plate which is mounted on a multi-axis adjustment device to provide feed movement in the focal-plane of the reflector to measure scanned beam performance. The adjustable mechanisms provides a 5-in movement in any desired direction in the focal-plane.

## IV. TEST RESULTS

Measured results of the components and the XMBA assembly are described in this section. The Potter horn has measured return loss of better than 30 dB and peak crosspolar levels of less than  $-36$  dB (relative to copolar peak gain) over the 43.5–45.5 GHz band. Fig. 8 shows the circularly polarized patterns of the radiating element assembly (Potter horn, polarizer, and transformer) measured using a rotating linearly polarized source antenna. The axial ratio of the element is less than 0.80 dB over the illumination region of the reflector ( $\Theta = \pm 16.1$  degrees). Active patterns of the central element with six edge elements of the septet being match-terminated are very similar to the isolated element patterns shown in Fig. 8. This indicates that the mutual coupling effects in the septet array are negligibly small. Test results of the waveguide intercon have shown that the measured return loss at input and output ports is better than 20 dB, the insertion loss is less than 0.11 dB, and the phase difference among the seven channels is less than 20 degrees.

The PAC modules have measured return loss of better than 20 dB. To measure the performance of the passive BFN, dummy loads of both full-height and half-height are used.

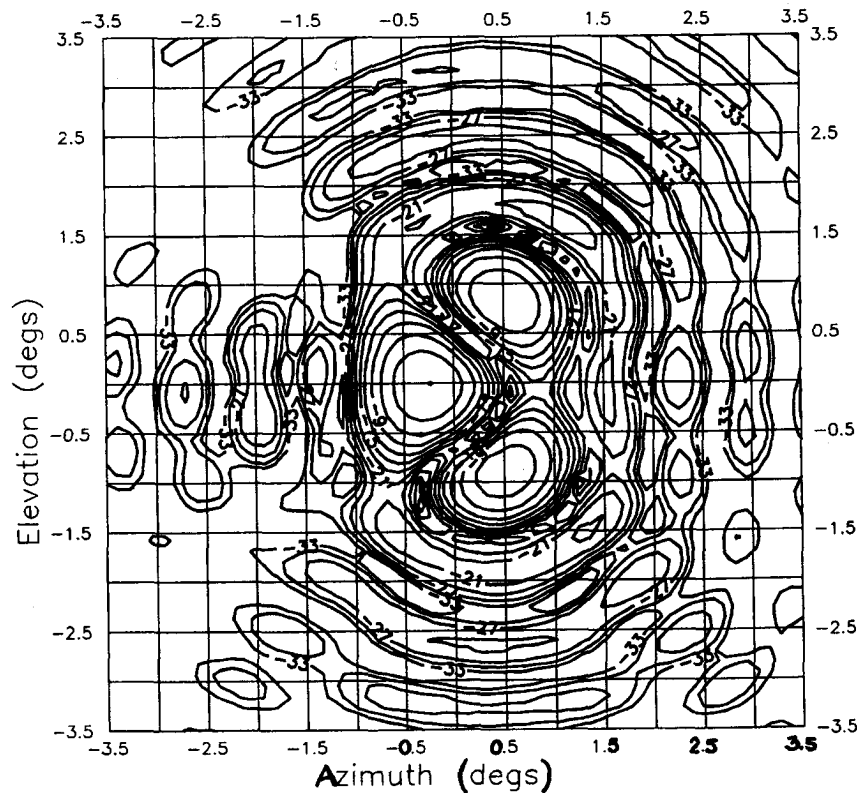


Fig. 11. Measured adapted beam-gain contours of the XMBA for two jammers located at .6 degrees and 1.6 degrees along azimuth.

The half-height waveguide loads are required to terminate the isolated ports of the branch-line couplers, and these loads are integral to the BFN. The full-height waveguide loads are external to the BFN and are required to terminate six of the seven input ports of the BFN during testing. The output combining port has a return loss of better than 24 dB. Measured output amplitude and phase variations across the output ports and over the band are 0.38 dB and 19.3 degrees, respectively. Insertion loss of the BFN is measured as 0.19 dB. Measured output return loss of the feed assembly is better than 20 dB. A good agreement is achieved between the measured and designed excitations with maximum difference of 0.54 dB in amplitude and 1.3 degrees in phase.

The electrical performance of the XMBA has been measured in the Spar's compact range facility. The compact range uses a crosspolar compensated dual-reflector system (side-fed offset Cassegrain) with less than  $-40$  dB crosspolar levels. It has a quiet-zone of  $5.5 \text{ m} \times 5.0 \text{ m} \times 6.0 \text{ m}$  (width  $\times$  height  $\times$  length).

#### A. Composite Beams

All the composite or quiescent beams-gain contours are measured with septet feed array with tapered excitations. They have been measured by raster scanning the XMBA over a large window of 6 degrees  $\times$  6 degrees along azimuth and elevation axes to measure the worst-case sidelobe and crosspolar levels. The amplitude and phase settings of the PAC units are adjusted as per the composite beam excitation values. Measured copolar (RHCP) and crosspolar (LHCP)

gain contours of the XMBA are shown in Fig. 9(a) and (b), respectively. The skirt region in the figures is shown as a dotted circle with 3.0-degree diameter. The peak gain of the antenna, obtained by integrating the measured copolar and crosspolar contours and subtracting the polarizer and horn losses, is 43.8 dBic. The half-power beam width of the XMBA is measured as 0.95 degrees. Sidelobe levels outside the skirt region in Fig. 9(a) are better than  $-30$  dB relative to peak gain. The measured gain contours agree well with the computed gain contours. Measured crosspolar levels as shown in Fig. 9(b) are lower than  $-26$  dB (relative to the copolar peak) inside the skirt region and are  $-49$  dB outside the skirt region.

The scanned beam patterns of the XMBA are measured by moving the feed array in the focal plane using the adjustable vernier mechanisms. Fig. 10 shows measured copolar gain contours when the beam is scanned 3.4 degrees towards east. Sidelobe levels outside the skirt region are better than  $-25$  dB relative to peak gain and the scan loss is 0.30 dB. The crosspolar levels for the east beam are measured as  $-32$  and  $-49$  dB inside and outside the skirt region.

#### B. Adapted Beams

Adapted beam performance of the XMBA has been measured for different jamming scenarios using the element beam approach. The amplitude and phase weights of the closest element(s) of the septet to the jammer location(s) are only adjusted to create a single or multiple nulls. Fig. 11 shows measured patterns of the XMBA when the beam is adapted for

two jammers located at 0.6 and 1.6 degrees along the azimuth direction. Null depths are measured as 32 dB at 0.6 degrees and 30 dB at 1.6 degrees. Adapted patterns for the scanned beams have also been measured and realize a minimum null depth of 31 dB.

The XMBA test results have shown that it has very low sidelobe levels and extremely low crosspolar levels in the critical region outside the main beam skirt and has very low scan loss of 0.38 dB over the  $\pm 4$  beamwidths coverage region.

## V. CONCLUSIONS

Breadboard development results of a 45 GHz adaptive MBA with wide-angle coverage have been presented. The use of enhanced feed concept to achieve high adjacent beam overlap, low sidelobe levels, and beam adaptability of the MBA has been demonstrated. Measured results have demonstrated that the XMBA has high adjacent beam overlap of 2.8 dB as well as low sidelobe levels and low scan losses. Measured crosspolar levels are extremely low in the critical regions, and the XMBA adapted patterns have null depths of better than 31 dB. The measured contours of the composite beam as well as adapted beams are in close agreement with the theoretical contours. The breadboard design of the XMBA is amenable to flight antennas for EHF Satcom.

## ACKNOWLEDGMENT

The authors would like to thank B. Benton of Electromagnetic Sciences Inc., Atlanta, and J. Wang, J. Kopal, and M. Zaidi of Spar Aerospace Ltd. for their contributions. The authors are indebted to the reviewers for their valuable comments and suggestions which have helped to improve the technical contents of the paper.

## REFERENCES

- [1] K. S. Rao, G. A. Morin, and K. K. Chan, "Multiple beam antenna design for the Canadian EHF Satcom," in *IEEE Antennas Propagat. Symp.*, 1991, pp. 1682-1685.
- [2] K. S. Rao, M. Tang, and K. K. Chan, "Exploratory multiple beam antenna design," Spar, Ste-Anne-de-Bellevue, P.Q., Canada, Contract Report Submitted to Canadian DND, Oct. 1990.
- [3] S. Stein, "On cross coupling in multibeam antennas," *IRE Trans. Antennas Propagat.*, vol. AP-10, p. 430, July 1962.
- [4] E. Dufort, "Optimum low sidelobe high crossover multiple beam antennas," *IEEE Trans. Antennas Propagat.*, vol. AP-33, no. 9, p. 946, Sep. 1985.
- [5] J. P. Montgomery, D. L. Runyon, and J. A. Fuller, "Large multibeam lens antennas for EHF Satcom," in *IEEE Military Microwave Conf.*, no. 2, Oct. 1988, pp. 369-373.
- [6] P. Ingerson and C. A. Chen, "The use of non-focussing aperture for multibeam antenna," *IEEE Antennas Propagat. Symp.*, 1983, pp. 330-333.
- [7] K. S. Rao and H. J. Moody, "Modelling of shaped beam satellite antenna patterns," *IEEE Trans. Antennas Propagat.*, vol. 35, pp. 639-642, June 1987.
- [8] G. S. Gupta, M. Tang, K. S. Rao, and C. K. Mok, "Design and trade-off study for Intelsat 7 C-Band antenna system," *SBMO Int. Microwave Symp.*, São Paulo, Brazil, July 1989, pp. 207-212.
- [9] K. S. Rao, "A template for shaped beam satellite antenna patterns," *IEEE Trans. Antennas Propagat.*, vol. AP-36, pp. 1633-1637, Nov. 1988.
- [10] G. S. Gupta, "Potter horn analysis and synthesis software," Spar, Ste-Anne-de-Bellevue, P.Q., Canada, Rep. RML-009-88-010, Jan. 1988.



**K. Sudhakar Rao** (M'83) was born in Tenali, Andhra Pradesh, India, on July 15, 1951. He received the B.Tech. degree in electronics and communications engineering from the Regional Engineering College, Warangal, India, in 1974, the M.Tech. degree from the Indian Institute of Technology, Kharagpur, with a specialization in microwave and radar engineering, in 1976, and the Ph.D. degree in electrical engineering from the Indian Institute of Technology, Madras in 1980.

From 1976 to 1977, he was a Technical Officer with the Electronics Corporation of India Limited, Hyderabad, where he worked on LOS and TROPO communications antennas. From 1977 to 1980, he was with the Indian Institute of Technology, Madras, as a Research Assistant and worked on the application of GTD techniques for horn antennas. He worked with the Electronics and Radar Development Establishment (LRDE), Bangalore, from 1980 to 1981, as a Scientist, and was involved with the design and analysis of phased array radar antennas. During 1981 and 1982, he worked with the University of Trondheim, Norway, on earth station antennas and had a Postdoctoral Fellowship from the Royal Norwegian council for Scientific and Industrial Research (NTNF). He spent one year, 1982 to 1983, with the University of Manitoba, Winnipeg, where he worked as a Research Associate on low sidelobe sandwich wire antennas. He has been with Spar Aerospace Limited, Ste-Anne-de-Bellevue, Québec, Canada, since 1983, where he is currently the Staff Scientist in the Satellite Systems Division. His current research interests include satellite communication antennas, active antennas, mobile personal communications, and antenna measurements. He has published over 50 journal and conference papers in the area of microwave antennas.



**Gilbert A. Morin** (S'86-M'87) received the Bachelor of Applied Sciences degree in engineering physics from the Ecole Polytechnique de Montréal, Canada, in 1977, and the Master of Applied Sciences and Ph.D. degrees, both in electrical engineering, from the University of Toronto, Canada, in 1980 and 1987, respectively. During his graduate studies, he worked in the field of wire antennas in free space and in the ionosphere.

In 1987, he joined the Defence Research Establishment, Ottawa, Canada, and has been working in the field of reflector and lens antennas for space applications.



**Minh Q. Tang** was born in Saigon, Vietnam, in 1953. He studied physics and mathematics from 1976 to 1978 at the University of Winnipeg, Manitoba, Canada. He received the B.S. degree in electrical engineering from the University of Manitoba, Winnipeg in 1981. From 1981 to 1982 he spent a year doing graduate studies at the University of Manitoba.

He has been with the Spar Aerospace Limited, Ste-Anne-de-Bellevue, Québec, Canada, since 1983, where he is currently a Senior Member of Technical Staff in the Antenna Department. His current interests are satellite antenna design and software development.



**Sylvain Richard** (M'93) received the B.S. degree in electrical engineering from Laval University, Québec, Canada, in 1984.

Since 1984, he has been working for Spar Aerospace Ltd. on various satellite antenna projects. He is a Senior Development Engineer of the Antenna Engineering Department. His research interests include beamforming networks (BFN) and BFN component design, as well as multipactor and PIM testing.



**Kwok Kee Chan** received the B.Eng. degree from Imperial College, London, in 1970 and the M.Eng. and Ph.D. degrees from McGill University, Montréal, in 1971 and 1973, respectively.

After graduation, he spent a year at the Canadian Center for Remote Sensing in Ottawa developing an airborne scatterometer. From 1974 to 1982 he worked at Spar Aerospace where he developed, designed, and tested satellite and ground-based antenna systems. Since 1983, he has served as a consultant to both industrial and government

organizations in North America and Europe.